Hindawi
Science and Technology of Nuclear Installations
Volume 2022, Article ID 7265821, 15 pages
https://doi.org/10.1155/2022/7265821

Research Article

Study on the Dispersion of Radionuclides under Different Hydrological Conditions of Spent Fuel Shipping in Daya Bay

Liwei Chen,[1,2,3] **Weihua Chen**,[1] **Jiazhen Lin**,[1] **Chunhua Chen**,[2] **Yalin Luo**,[1] **and Longlong Tao**[2]

[1]*State Key Laboratory of Nuclear Power Safety Monitoring Technology and Equipment, China Nuclear Power Engineering Co., Ltd, Shenzhen 518172, China*
[2]*Institute of Nuclear Energy Safety Technology, Hefei Institutes of Physical Science, Chinese Academy of Sciences, Hefei, Anhui 230031, China*
[3]*School of Computer Science and Technology, Hefei Normal University, Hefei, Anhui 230601, China*

Correspondence should be addressed to Chunhua Chen; chunhua.chen@inest.cas.cn

Received 23 April 2022; Revised 24 May 2022; Accepted 25 May 2022; Published 10 June 2022

Academic Editor: Peter Ivanov

The radionuclide dispersion in coastal water is mainly controlled by the water flow and tidal effect. Tracing and analysis of radioactive pollutant dispersion in coastal water can predict distribution of radionuclide under marine transportation accident of spent fuel. In this work, factors such as continuous emission, radioactive decay, and water depth are considered, and a hydrodynamic model of radionuclide dispersion based on shallow water equations is established to simulate the dispersion of the radioactive pollutant in coastal waters under different hydrological conditions. As far as the characteristics of the radionuclide dispersion in coastal water are concerned, the simulation of pollutants by the hydrodynamic model is in good agreement with the work of Bailly du Bois et al., which validated the correctness of this model. The model has been applied to simulate the distribution of radionuclides in coastal water following a marine transport accident of spent fuel near Daya Bay Nuclear Power Plant in China. The simulation reveals that the distribution features are significantly affected by different hydrological conditions. In addition to limiting the diffusion range, the vortex effect can also cause the accumulation of radionuclides near the vortex, which helps to provide more practical information for nuclear emergency decision makers.

1. Introduction

From March to April 2011, about 80 percent of the radioactive contaminants released were discharged into the ocean except for the deposited radionuclides from the atmosphere due to the Fukushima Daiichi Nuclear Power Plant accident, which caused persistent contamination of the ocean [1, 2]. Pollution occurs in two ways, direct discharge into the ocean and deposits from the atmosphere to the ocean surface [1]. With the development of nuclear power plant in China, the highway transportation cannot meet the current scale of spent fuel transportation, and the sea-road combined transportation is the main way to relieve transportation pressure [3]. Moreover, with the rapid development of floating nuclear power plants, coastal nuclear power plants, or marine transportation of spent fuel, the increased risk of radioactive contamination accidents is caused by extreme events such as storms, tsunamis, floods, and collisions [4]. The radioactive pollutant would be transported by wave on free surface flows (rivers, streams, seawater, etc.) after the coastal nuclear accident. Under accident conditions, the leakage of radioactive materials will cause radiation hazard to the offshore area. Furthermore, if leakage accidents are not controlled, the effluent may return to the coastal regions without being sufficiently diluted, so it can contaminate areas for agriculture, fishing grounds, or beaches [5].

Radionuclide dispersion simulation can intuitively assess the harmful radiation under the nuclear accident condition and predict the distribution of the radioactive pollutant [6]. Marine radioactive contaminants in different scale are

generally simulated by marine radionuclide dispersion models. Kawamura et al.'s work used the particle random-walk model SEA-GEARN to simulate the oceanic spreading of ^{131}I and ^{137}Cs [7]. A high resolution regional ocean model was used to simulate the ^{137}Cs concentration from March to May by Tsumune et al.'s work [8]. State-of-the art dispersion models were applied to simulate ^{137}Cs dispersion from Chernobyl Nuclear Power Plant disaster fallout in the Baltic Sea and from Fukushima Daiichi Nuclear Power Plant releases in the Pacific Ocean after the 2011 tsunami [1]. A hydro-sedimentary model was proposed to investigate the radionuclide dispersion and to analyze the potential hazard to marine ecosystem under the leakage accident condition in Dufresne et al.'s work [9]. The dispersion of radionuclides in coastal water was simulated by Lagrangian model and Euler model in Zichao Li et al.'s work, and the characteristics of radionuclide dispersion were revealed [10]. However, offshore radionuclide dispersion simulations are characterized by complex terrain and tidal cycles, and the dispersion of leaked radionuclide on a free surface would be affected by water flow and tidal cycle.

This paper assumes that a marine transportation accident of spent fuel occurs within 12 hours near the Daya Bay Nuclear Power Plant (DBNPP), and provides reasonable suggestions for early nuclear emergency decision makers under different hydrological conditions under marine transportation accidents. Tidal effect was mainly considered for the scenario hypothesis in Section 2.1 since the calculation domain is between 1 km and 50 km and the simulation time is between 1 h and 2 days [11]. Compared with the existing models, the shallow water equations as a powerful tool can describe the domain whose depth is considered to be shallow compared with the horizontal scale in the scenario hypothesis, being particularly useful when modeling pollutant dispersion in coastal water and offering a large potential to increase the efficiency of the simulation [12]. Considering the efficiency for nuclear emergency response, the process of radionuclide released under the marine transportation accident on a free surface flow was simulated by the hydrodynamic model based on shallow water equations, which can provide nuclear emergency decision makers with the reference basis as soon as possible. The shallow water equations were applied to solve the flow field, and the radioactive pollutant concentration was estimated by adding a concentration equation, so as to provide more actual information of the radionuclide distribution near offshore.

2. Materials and Methods

Radioactive contaminants that leak into seawater are transported by water flow and tide motion. By coupling the shallow water equations with the radionuclide concentration equation, the diffusion of radioactive contaminants on free surfaces can be estimated accurately. The simulation procedure of the radionuclide dispersion in coastal water consists of three steps (as shown in Figure 1): scenario hypothesis (including hydrology and topography of Daya Bay Area (DBA), accident scenario of marine transportation, and the way radionuclides are released); modeling of radionuclide dispersion in coastal water (including shallow water equations, radionuclide concentration equation) and validation; and simulation of radionuclide dispersion in coastal water. Hydrological boundary conditions were assumed based on hydrology and topography of DBA. Source term boundary conditions were assumed base on accident scenarios of marine transportation and the way radionuclides are released. Finally, radionuclide dispersion was simulated in coastal water based on the proposed model through the simulation configuration in Section 2.4. In addition, the open source software OpenFOAM 4.1 was used to simulate radionuclide dispersion in this work.

2.1. Scenario Hypothesis

2.1.1. Hydrology and Topography of Daya Bay Area. Daya Bay Area (DBA), located on the north side of South China Sea, is semi-enclosed shallow water bay with an area of about 600 km^2, and coastline of the DBA has characteristics of twists and turns. There are many islands, such as Xuzhou islands, central islands, and Xiaolajia island, lying at the central and western end of the DBA. During the tide, the water flows from the central island to the northwest to the Dapeng'ao area, with an average velocity of about 0.5 m·s^{-1} [13]. In hydrodynamic model based on shallow water equations used in this work, the distribution of flow field is the main factor affecting the spread of radionuclides; the incompressible, Newtonian, and immiscible fluids were assumed in this work; and isothermal state of ambient temperature was assumed under the tidal flow.

2.1.2. Accident Scenario of Marine Transportation of Spent Fuel. Daya Bay Nuclear Power Plant (DBNPP) is located at Dapeng'ao area of the DBA, and reprocessing plant of spent fuel lies to the northwest of China. Marine transportation of spent fuel is an important way to relieve road transportation stress; spent fuel vessel will be transported by ships from DBNPP to reprocessing plant during marine transportation. There are two routs of marine transportation of spent fuel in China: one is an offshore route near the DBA, and the other is the ocean route to the east of Taiwan. With consideration of the hydrological characteristic and emergency rescue in coastal water, five basic principles of transportation routes are followed: (1) to improve emergency response effectiveness, the routes should be close to shore; (2) to salvage the spent fuel vessel under the accident condition, the water depth must be less than 200 m; (3) to reduce the hazard of accident, fishing grounds, restricted areas, and heavy traffic areas need to be avoided [15]; (4) the weather is fine under the marine transportation accident, and wind-driven effect is not considered since the wind has no strong influence on radionuclide diffusion [11]; (5) originating the large scale ocean circulation (for instance, the Kuroshio current) is not considered.

To study potential hazards of radionuclides released under the accident conditions of marine transportation of spent fuel, such as drop, collision, and fire scenario, the

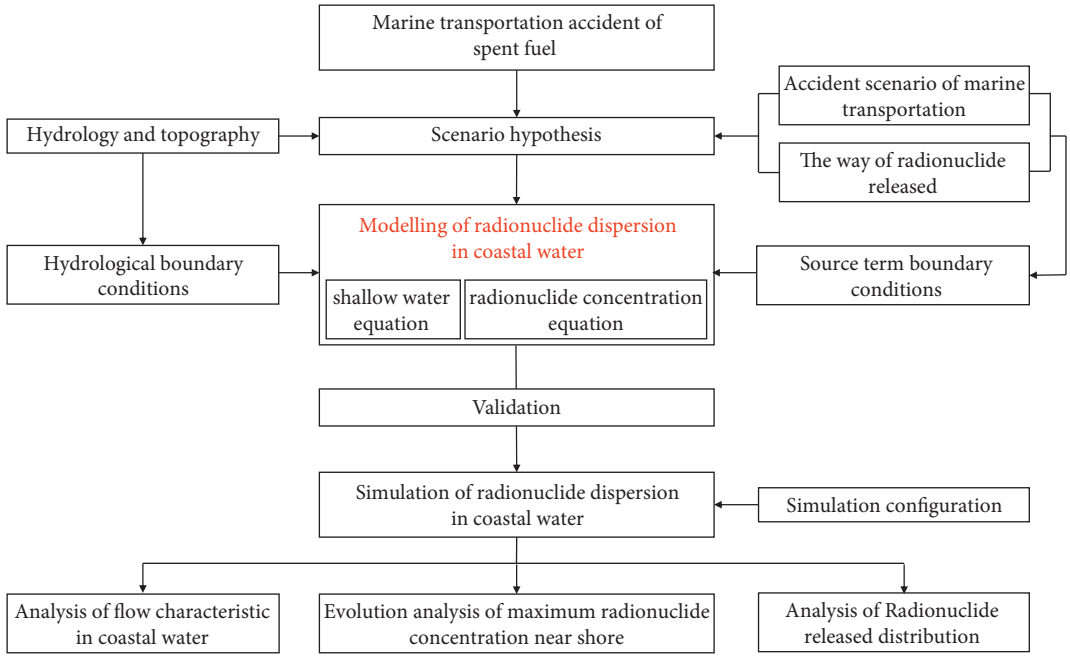

Figure 1: Simulation procedure of radionuclide dispersion in coastal water.

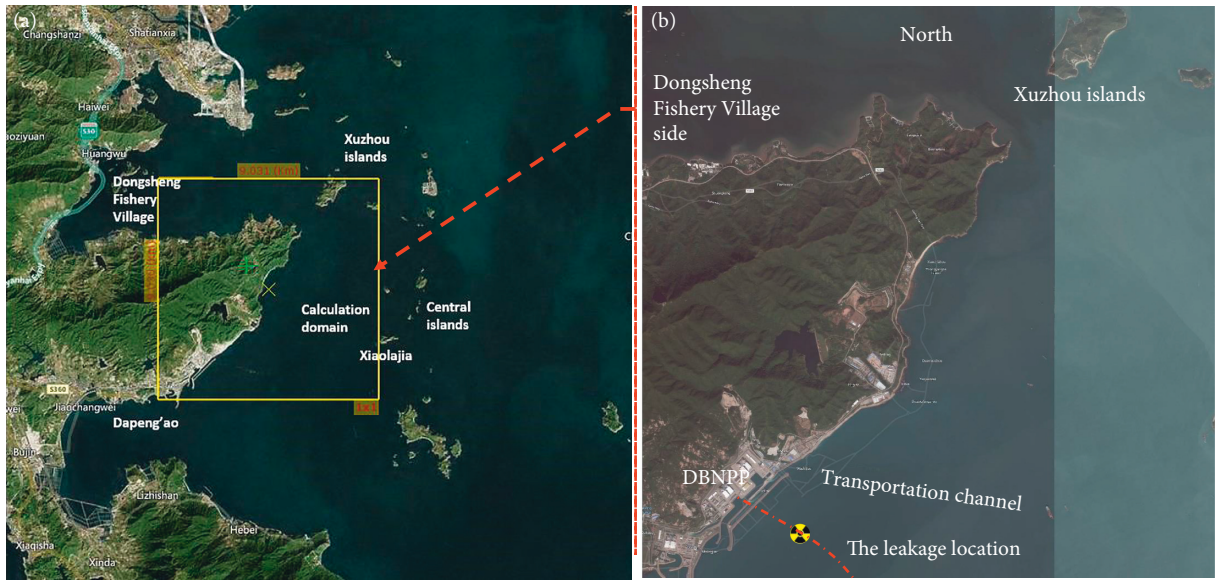

Figure 2: Accident scenario of marine transportation in DBA. (a) Real terrain. (b) Terrain model.

accident scenario was selected to perform the simulation with the following considerations: (1) a spent fuel carrier sailed out of the bay along the southeast route and hit rocks; (2) the radionuclide release from the vessel is caused by drop and impact after the accident; (3) various kinds of radionuclides could be emitted from severe marine nuclear accidents, among which ^{137}Cs is representative of volatile, dissolved fission products [16]; (4) the effect of water flow on ^{137}Cs dispersion characteristics is simulated, and potential hazard of radionuclides released into coastal environment is discussed. The spent fuel vessel falls into the bottom of the coast water below a surface since the ship hit a rock.

The real terrain of DBA from Google Maps, about 9 km × 9 km area, was used for simulation as shown in Figure 2(a), and a terrain model was obtained by Google Maps as shown in Figure 2(b). The leakage point of radionuclide is 500 m from the DBNPP on the transportation route.

2.1.3. The Way Radionuclides Are Released under the Accident Condition. The impact of accident brings about the deformation of the sealing rings of spent fuel vessel, which leads to the leakage of radionuclides from the container into the aquatic environment of coastal waters [17]. The leaked radionuclides were assumed to be point source under the accident condition, and continuous and uniform release of leaked radionuclides was taken into account. In addition, the accident scenario in offshore has tidal characteristic, and the

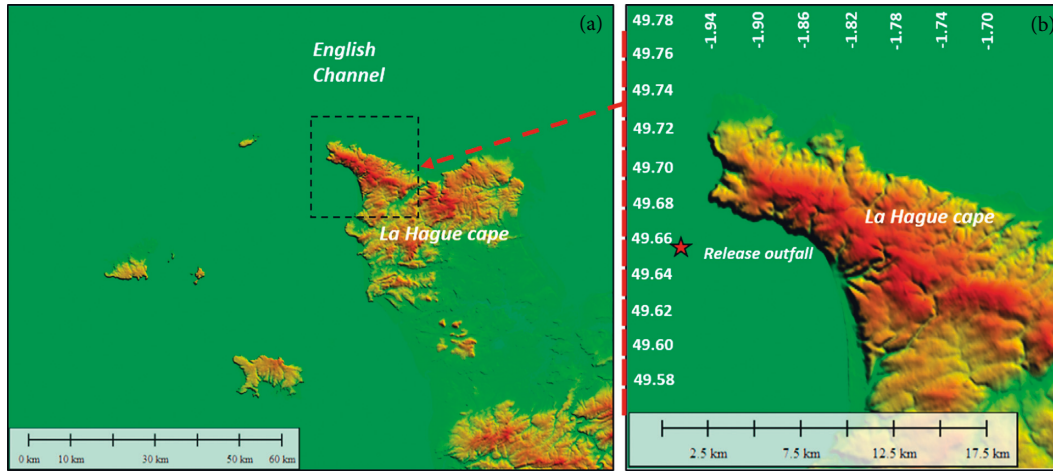

FIGURE 3: Terrain of the Cap de La Hague. (a) Simulation region in Bailly du Bois et al.'s work. (b) Region of release outfall near the coastline.

radionuclide dispersion on a free surface would be transported by the tidal flow first and then dispersed to environment gradually due to complexity terrain and tidal flow during the transportation.

Two parts for modeling radionuclide dispersion in coastal water are shown in Figure 1, which are the solution of water flow field and the solution of the radionuclide concentration. The tidal flow tracking by shallow water equations was applied to solve the flow field in coastal water. The distribution of radionuclide was obtained by the radionuclide concentration equation, the mass conservation equation, and the momentum conservation equation. 12-hour continuous release of the ^{137}Cs below the free surface was assumed; the leakage point is 500 m from the DBNPP on the transportation route, located at (4500, 3000) of the terrain model; and the leakage rate of ^{137}Cs is about 2×10^9 Bq·m^{-3}·s^{-1}.

2.2. Governing Equations. In order to describe characteristic of shallow water flow in coastal water, the water flow fields in coastal water under marine transportation accident were solved by the shallow water equations, which are the mass conservation equation and the momentum conservation equation [18].

The mass conservation equation is as follows:

$$\frac{\partial h}{\partial t} + \nabla \cdot U = 0. \tag{1}$$

The momentum conservation equation is as follows:

$$\begin{aligned} \frac{\partial \mathbf{U}}{\partial \mathbf{t}} + \nabla \cdot (\mathbf{u} \otimes \mathbf{U}) &= \nabla \cdot \boldsymbol{\tau} - \nabla\left(\frac{\mathbf{g}\mathbf{h}^2}{2}\right) + \mathbf{S}_b + \mathbf{S}, \\ \boldsymbol{\tau} &= \mu\left(\nabla \cdot \mathbf{U} + \nabla^T \cdot \mathbf{U}\right), \\ \mathbf{S} &= \boldsymbol{\tau}_c + \frac{\boldsymbol{\tau}_s}{\rho} + \frac{\boldsymbol{\tau}_b}{\rho}, \\ \boldsymbol{\tau}_c &= \mathbf{f}_c \mathbf{U},\ \mathbf{f}_c = 2\omega \sin\varphi, \end{aligned} \tag{2}$$

where h (m) is the total surface height, t (s) is the time, $\boldsymbol{u}$ (m/s) is the velocity vector, $\boldsymbol{U}$ ($=h\boldsymbol{u}$) is the conservation variable, g (m/s^2) is the gravity acceleration, τ (N/m) is the viscosity term, μ ($N{\cdot}s/m^2$) is the dynamic viscosity, $\boldsymbol{S_b}$ is the bottom slope term, ρ (kg/m^3) is the fluid density, $\mathbf{f_c}$ is the Coriolis force coefficient, ω (rad/s) is the angular rotation rate of the Earth, φ is the latitude, and τ_s and τ_b are the wind and bottom stresses, respectively.

During the process of radioactive pollutant dispersion, the released radionuclide from the leakage location would be governed by the flow field, and the radioactive decay is considered.

The radionuclide concentration equation is as follows:

$$\frac{\partial C}{\partial t} + \nabla \cdot (UC) = \nabla \cdot \left(\Gamma_c \nabla C\right) + S_C - \lambda C, \tag{3}$$

where C is the concentration of radionuclide (Bq/m^3), Γ_c is the diffusion coefficient (m^3/s), S_c is the source term (Bq/(m^3·s)), and λ is the radioactive decay factor.

2.3. Validation. Given the complexity of tidal cycle and coastline, the simulation of pollutant dispersion in the Cap de La Hague is considered as one of the most difficult tasks. Bailly du Bois et al.'s work provides validation data in the Cap de La Hague considering tidal cycle, which can be used for testing the reliability of our model against appropriate data [11], since the dispersion of the radioactive pollutant on a free surface is the key of this work. Figure 3(a) shows the terrain of the Cap de La Hague region in Bailly du Bois et al.'s work. The comparison of pollutant distribution evolution and concentration on a free surface was focused on the vicinity of coastline (as shown in Figure 3(b)), which applied to validate the correctness of the proposed model. In Figure 3(b), latitude and longitude are shown as ordinate and abscissa values, and release outfall location is described in detail.

From Bailly du Bois et al.'s work, the release time of tritium is from 16 : 10 to 17 : 50, the total activity is about 2.8×10^{13} Bq, and the velocity of water inlet is 5 m·s^{-1}. The detailed boundary conditions of calculation correspond to [11]. Figure 4 illustrates the tritium dispersion in both works; the left side is simulated from Bailly du Bois et al.'s work, and the right side is simulated from this work. Figure 4(a) shows

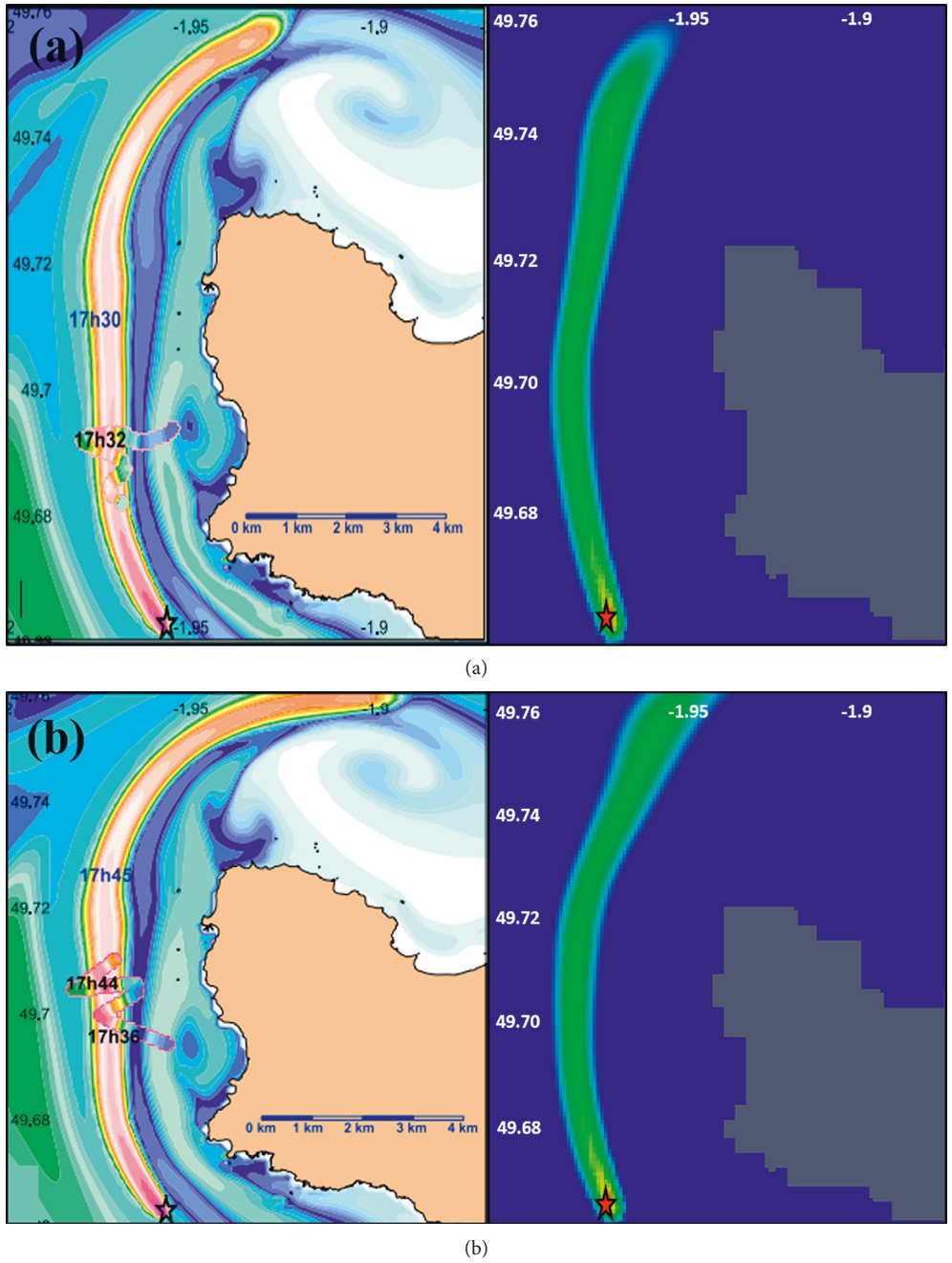

Figure 4: Tritium dispersion in the vicinity of Cap de La Hague. (a) $t = 17$ h 30. (b) $t = 17$ h 45.

$t = 17$ h 30, and Figure 4(b) shows $t = 17$ h 45 from Bailly du Bois et al.'s work. It can be seen that the direction of pollutant dispersion was from south to north first and then gradually shifted to east more than 1 hour after release time.

Table 1 illustrates the comparison of tritium concentration between Bailly du Bois et al.'s work and simulation in this work. The results of the two works indicate that the tritium dispersion and the concentration of the pollutant calculated by this work are in good agreement with Bailly du Bois et al.'s work. Although there is a little discrepancy result from the mesh difference and an imperfect representation of tidal currents, it can be seen that the pollutant distribution proves the agreement between both of them.

2.4. Simulation Configuration. Some preparatory work should be illustrated and explained firstly before the simulation. The terrain file as STL format was downloaded from Google Maps and imported to OpenFOAM. After loading the terrain file into the snappyHexMesh module, about 1×10^5 non-uniformly grids with 1.2-time expansion near the terrain boundary were used to mesh so as to guarantee the required grid resolution (as shown in Figure 5). A radionuclide concentration equation was added to the shallowWaterFoam solver and compiled. Water depth data originated from the Daya Bay hydrographic data [19], and the depth data interpolation to computational grid was made using the funkySetFields module. ^{137}Cs as source data was

Table 1: Comparison of tritium concentration.

Sampling points	Sampling time	Monitoring value ($Bq{\cdot}L^{-1}$)	Results in this work ($Bq{\cdot}L^{-1}$)	Fractional error (%)
(−1.961071, 49.691507)	17 : 30 : 00	6.56	5.31	19.1
(−1.958606, 49.692192)	17 : 31 : 00	6.13	5.18	15.5
(−1.959340, 49.694710)	17 : 34 : 00	6.78	5.31	21.7
(−1.964519, 49.696145)	17 : 36 : 00	6.63	5.33	19.6
(−1.966813, 49.705361)	17 : 44 : 00	6.63	5.47	17.5

created using the fvOptions module. The up and down boundaries were set as flow rate and water level, respectively. After finishing the grids and initial file, the calculation module was used to start the simulation by the updated solver with the time step as 1 min. The maximum permission value of $3.5 \times 10^4\ Bq{\cdot}m^{-3}$ was released in the sea under the accident condition [20]. With consideration of the effects of radiation hazard on the west of the GBA [21], the velocity of water flow is $0.5\ m{\cdot}s^{-1}$ along the northwestern direction.

3. Results and Discussions

In this work, the dispersion mechanism of ^{137}Cs in coastal water near DBNPP under the leakage accident conditions has been investigated through the proposed model. The following three aspects were analyzed: analysis of the water flow field, ^{137}Cs dispersion distribution, and contamination region beyond the maximum permission value.

In order to analyze the marine transportation in different water depth conditions, the detailed hydrological data as shown in Table 2 was obtained by Huizhou Daya Bay Economic Technological Development Zone Administrative Commission [19], and it indicates the average water depth in December and July. The water depth data based on Table 2 was interpolated to computational grid as shown in Figure 6, Figures 6(a) and 6(b) indicate the water depth in July and December, 2020, respectively.

3.1. Flow Characteristic in Coastal Water. Figure 7 shows the water flow field from $t = 0$ h to $t = 12$ h after radionuclide release under marine transportation accident in coastal water near DBNPP. The left and right side of each graph indicate the velocity vector of water flow on July 1 and December 1, respectively. The water flow field was analyzed through calculated data with the time step of two minutes. Obviously, it can be seen there are different flow fields under the different hydrological conditions on July 1 and December 1. The maximum velocity of water flow arises near the Xuzhou islands due to the narrow access between islands.

Figure 7 indicates that the flow direction in the vicinity of leaked point is mainly along the northeast. From Figures 7(a) and 7(b), the current direction on July 1 is the same as December 1 in 4 hours after the radioactive pollutant release under accident condition, although the current velocity has a little disparity. However, the current field would rise obviously differently between July 1 and December 1 from $t = 11$ h, especially for the current near the fishing grounds of Dongsheng Fishing Village as shown in Figures 7(c) and 7(d). In addition, the water flow from $t = 11$ h to $t = 12$ h on Dec. 1 is toward Xuzhou islands side.

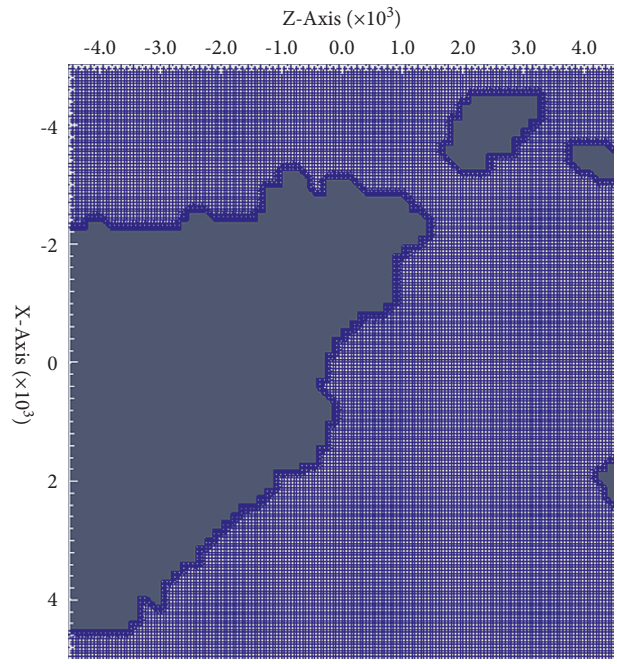

Figure 5: Grids of terrain in DBA.

Table 2: Hydrological data of Daya Bay in July and December, 2020.

Sites	Average water depth in July (m)	Average water depth in December (m)
Xuzhou islands	7.3	10.4
Xiaolajia	8.6	13.4
Dongsheng Fishing Village	6.6	8.2

3.2. Distribution of Radionuclides Released in Coastal Water. For detailed prediction of the most possible leakage trajectories under the accident to the environment through the water flow, simulation data of ^{137}Cs dispersion was used to analyze characteristic of dispersion and distribution with the time step of 6 hours. Figure 8 shows the radionuclide concentration field from $t = 0$ h to $t = 12$ h in coastal water near DBNPP. Dispersion process of ^{137}Cs continuous release at different times in 12 hours on a free surface is illustrated by Figures 8(a)–8(d). Figure 8(a) shows the distribution of ^{137}Cs at $t = 1$ h; Figure 8(b) shows the distribution of ^{137}Cs at $t = 4$ h; Figure 8(c) shows the distribution of ^{137}Cs at $t = 11$ h;

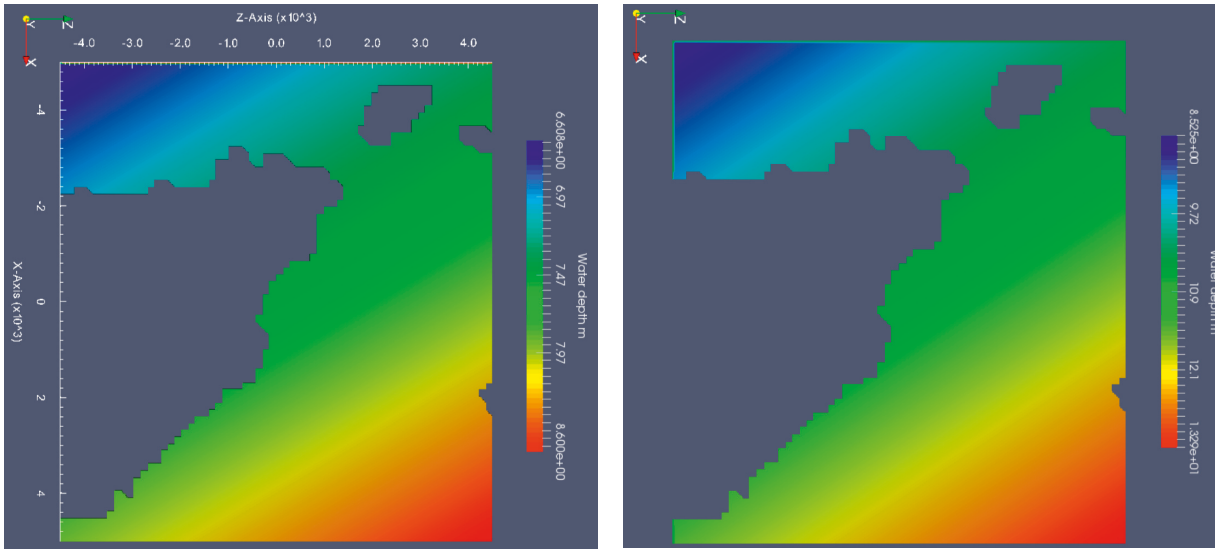

July (a) December (b)

Figure 6: Water depth data by interpolation based on Table 1. (a) July. (b) December.

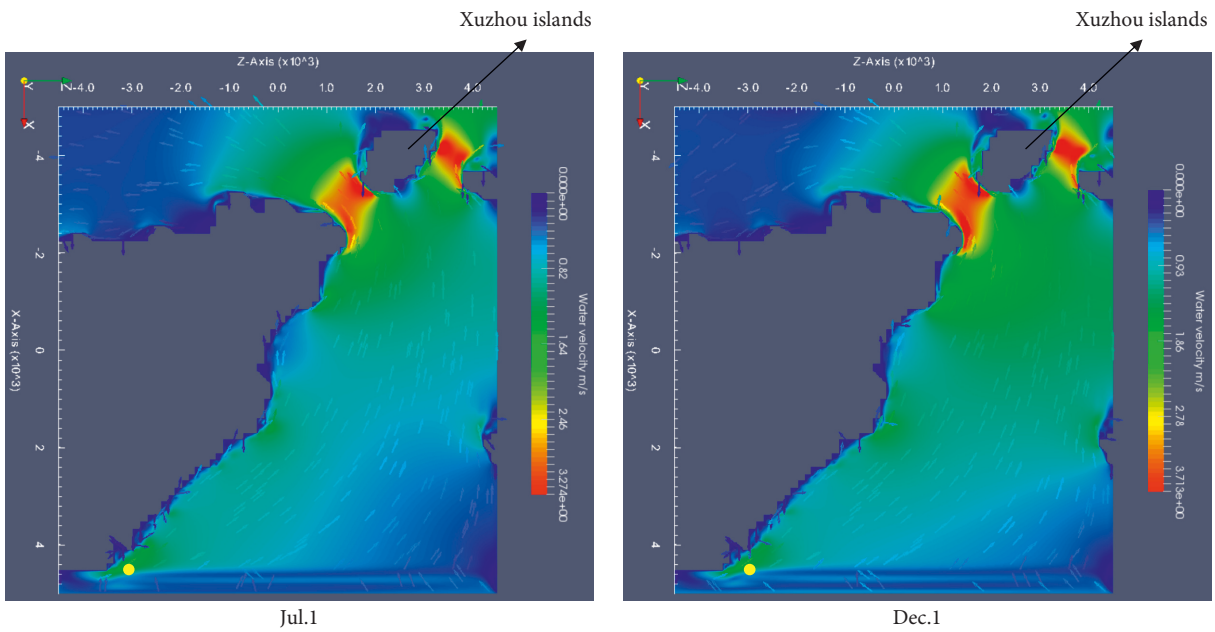

Jul.1 Dec.1

(a)

Figure 7: Continued.

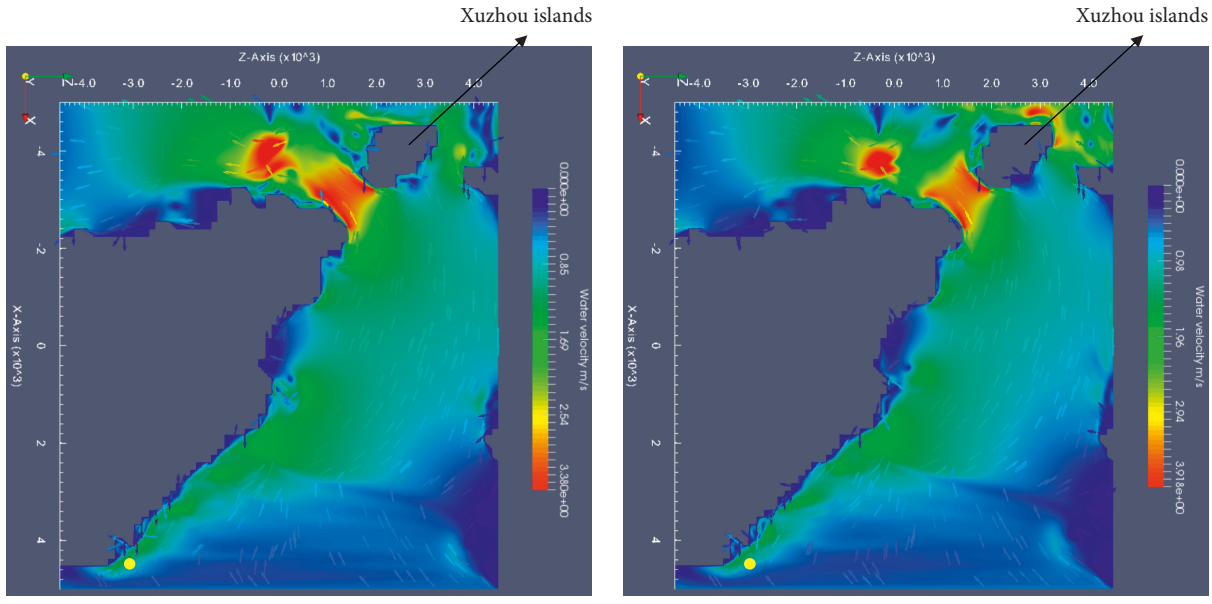

(b)

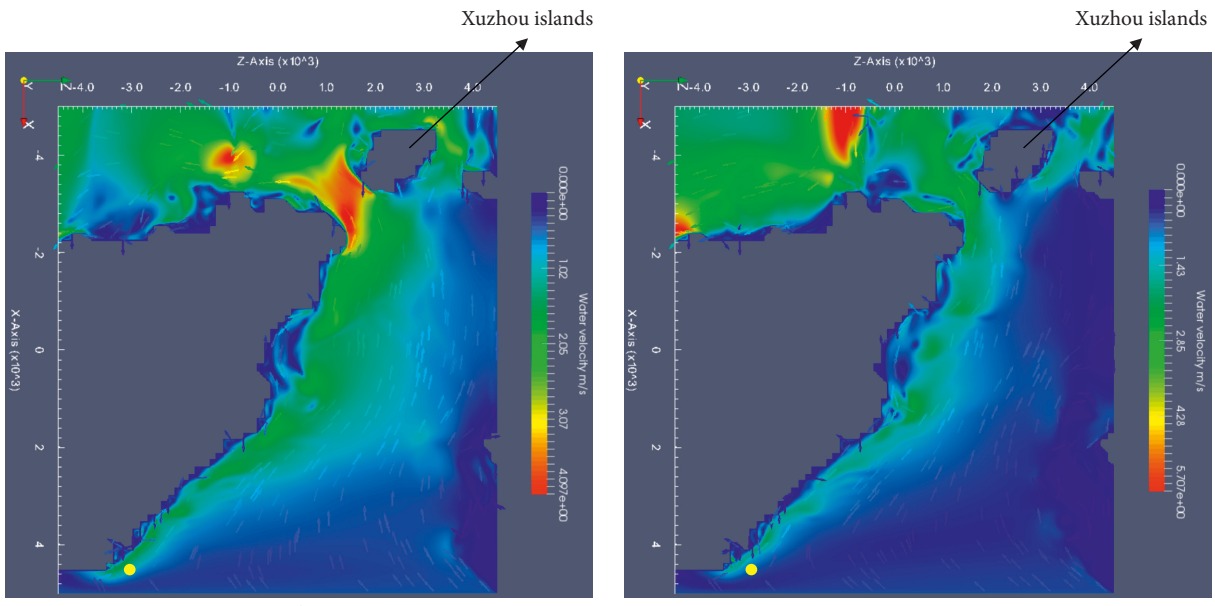

(c)

Figure 7: Continued.

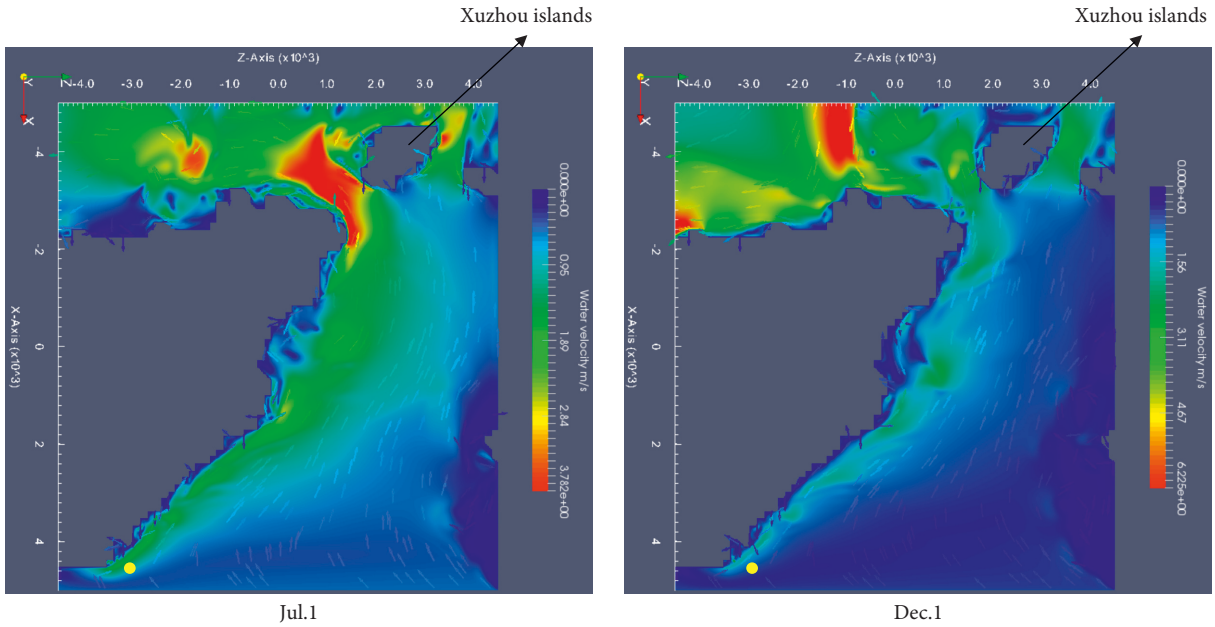

(d)

Figure 7: Simulation of the water flow field in 12 hours on Jul. 1 and Dec. 1, respectively. (a) $t = 1$ h. (b) $t = 4$ h. (c) $t = 11$ h. (d) $t = 12$ h.

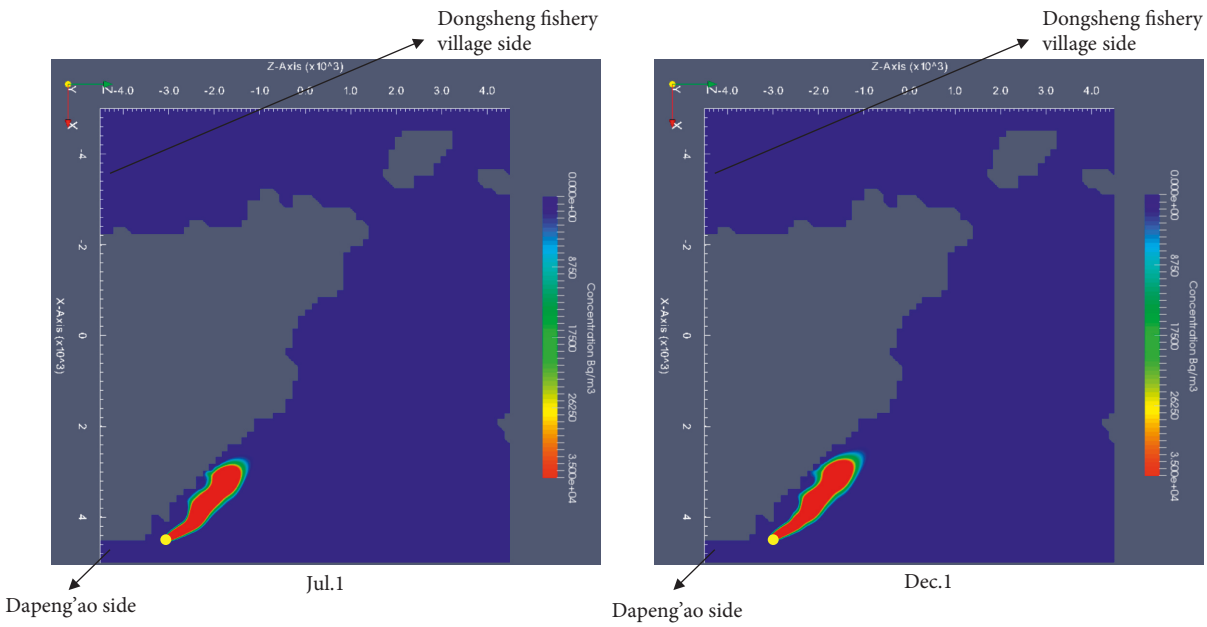

(a)

Figure 8: Continued.

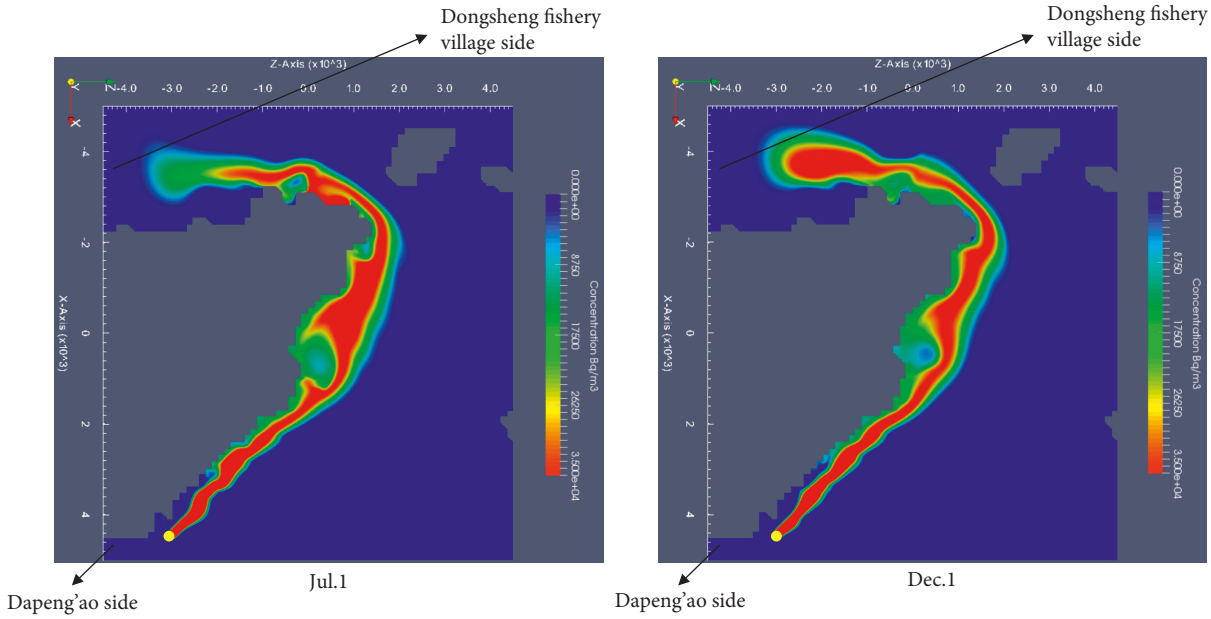

(b)

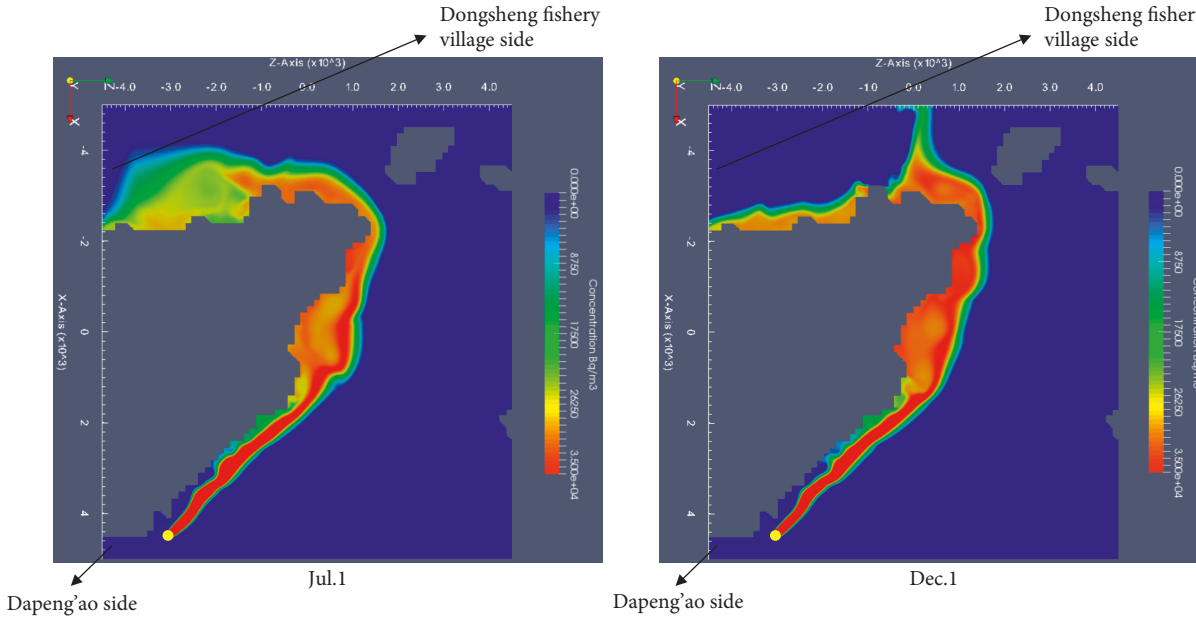

(c)

Figure 8: Continued.

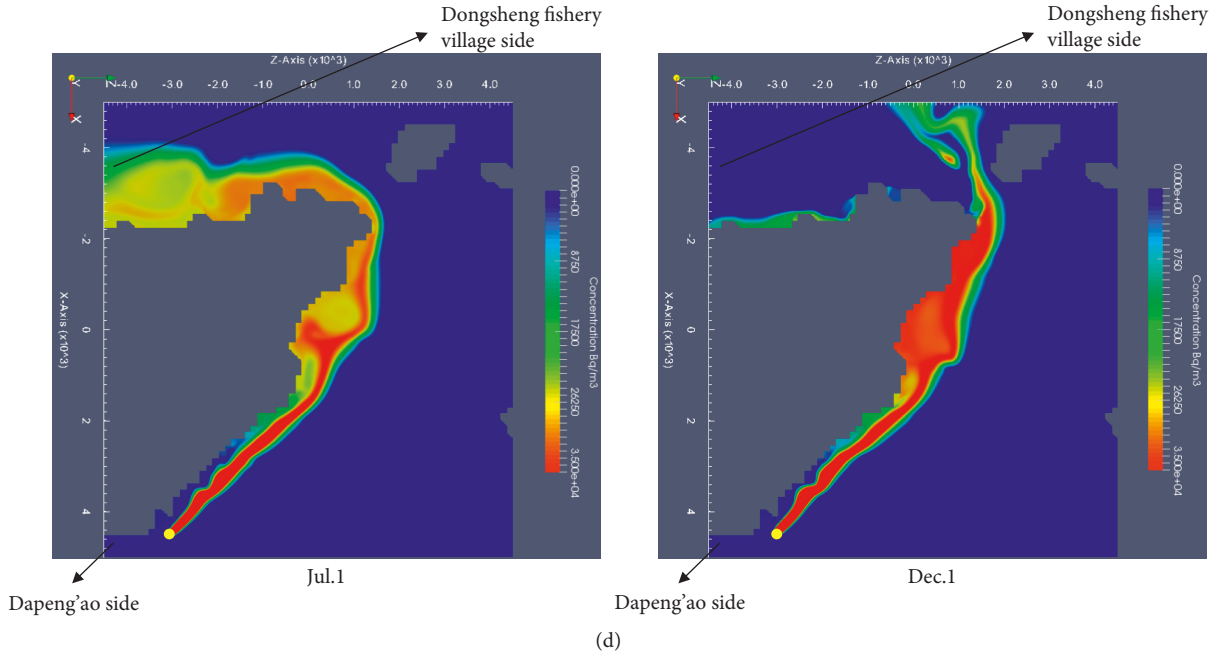

FIGURE 8: Simulation of the released ^{137}Cs concentration in 12 hours on Jul. 1 and Dec. 1. (a) $t = 1$ h. (b) $t = 4$ h. (c) $t = 11$ h. (d) $t = 12$ h.

Figure 8(d) shows the distribution of ^{137}Cs at $t = 12$ h. The left and right side of each graph indicate the ^{137}Cs distribution on July 1 and December 1, respectively. The red regions in the graph illustrate that the value of ^{137}Cs concentration is more than the maximum permission value in the seawater (3.5×10^4 Bqm^{-3}).

Figure 8 indicates that the direction of radionuclide dispersion in the vicinity of leaked point is mainly along the northeast. There is more and more radionuclide accumulation near offshore along the northeast direction, with no radioactive contaminant of water environment of Dapeng'ao under the boundary conditions in both times. In Figure 8, it is shown that the radionuclide spread toward the northeast direction gradually along the coast from $t = 0$ h to $t = 12$ h on July 1 and December 1, respectively. However, the distribution of radionuclide dispersion near the fishing grounds of Dongsheng Fishing Village is obviously different since $t = 4$ h between July 1 and December 1 according to Figures 8(b)–8(d).

First, compared with the distribution of ^{137}Cs on July 1, the region contaminated beyond the maximum permission value is larger on December 1, and this means that the fishing grounds of Dongsheng Fishing Village would be all affected by radioactive contamination in both times and the radionuclide would be detected earlier after the marine transportation accident on December 1 by simulation of the right side of Figure 8(b). Therefore, the fishing grounds of Dongsheng Fishing Village would be affected first by radioactive contamination in 4 hours after the marine transportation accident on December 1.

Second, due to current effect toward Xuzhou islands on December 1, it can be seen that the radionuclide spread toward the east direction first (as shown in the right of Figure 8(b)) and then change from west to northeast in the

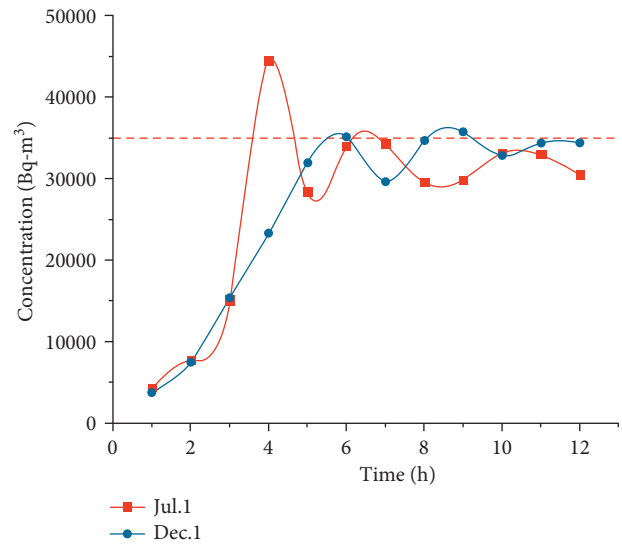

FIGURE 9: Evolution of maximum concentration of ^{137}Cs near shore in 12 hours.

fishing grounds of Dongsheng Fishing Village, and there is more and more radionuclide accumulation in the east shore near DBNPP on December 1 according to Figures 8(c) and 8(d). Moreover, compared with the radionuclide dispersion from $t = 11$ h to $t = 12$ h on July 1, there is less and less radionuclide accumulation in the fishing ground of Dongsheng Fishing Village on December 1 under the east flow effect near Xuzhou islands, which causes the region of radioactive contamination on a free surface to decrease rapidly as shown on the right sides of Figures 8(c) and 8(d), although a few radionuclides accumulate near offshore in Dongsheng Fishing Village. Therefore, the radioactive hazard of land

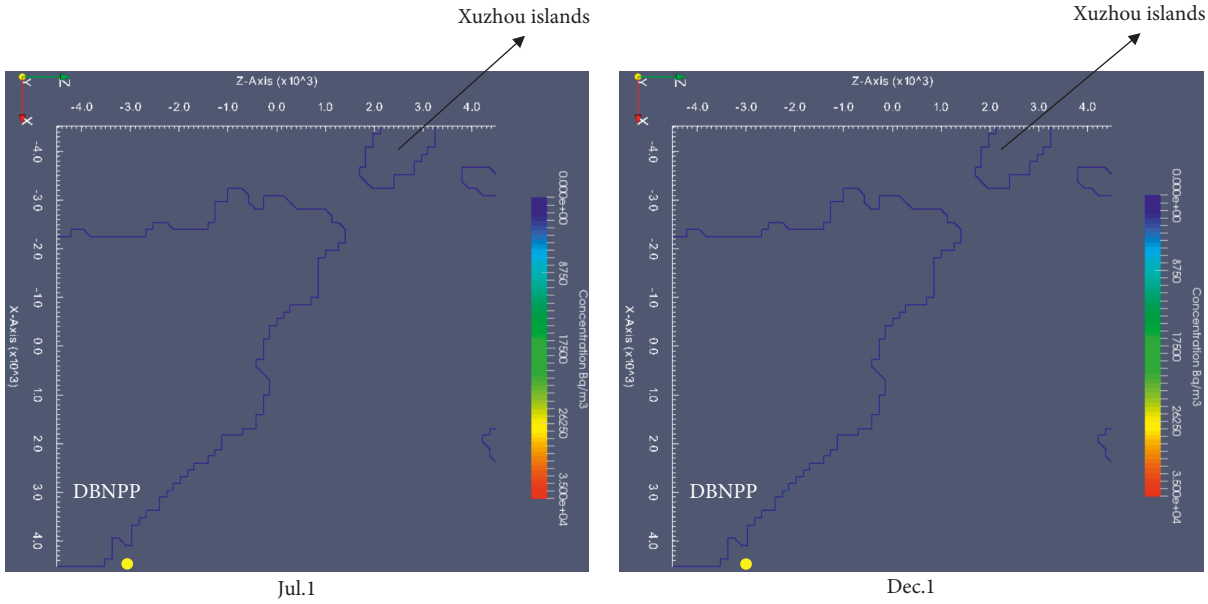

Jul.1 Dec.1

(a)

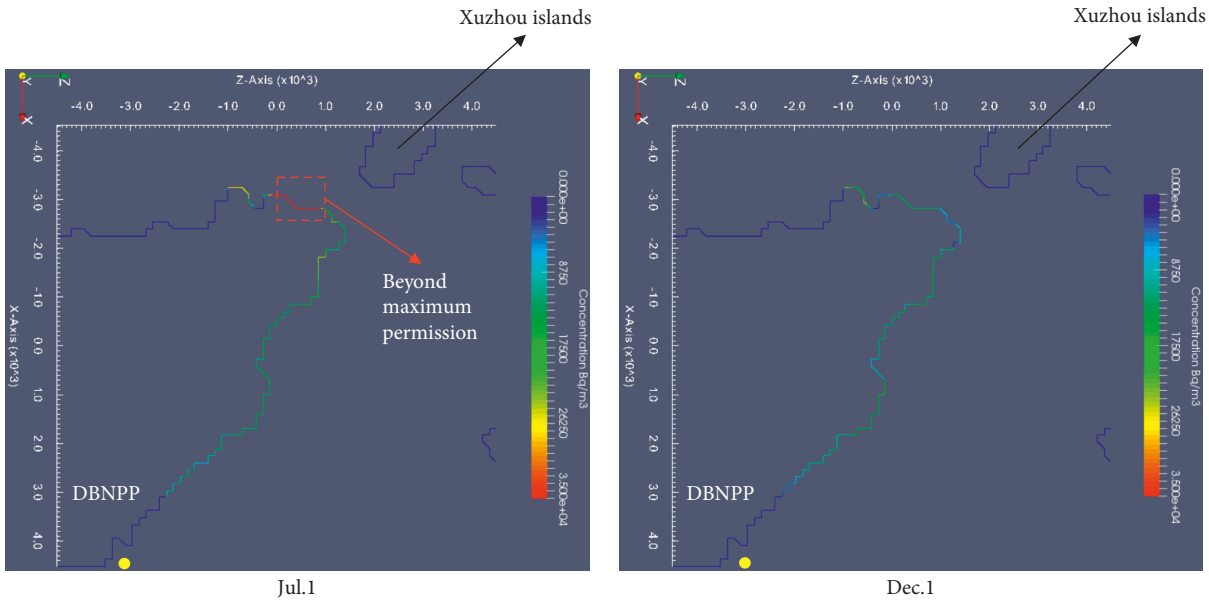

Jul.1 Dec.1

(b)

Figure 10: Continued.

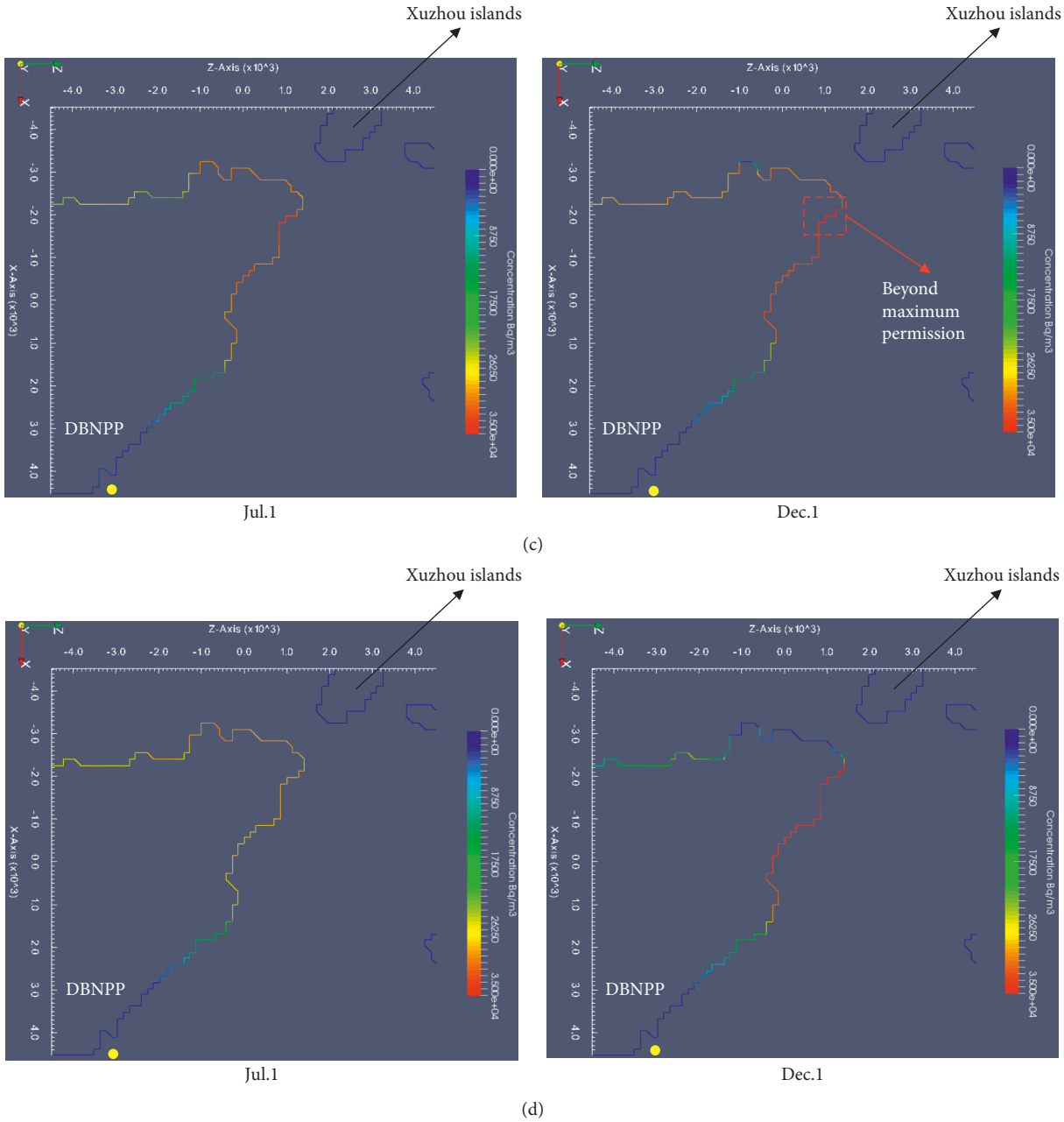

Figure 10: Maximum concentration of ^{137}Cs near shore in 12 hours on Jul. 1 and Dec. 1. (a) $t = 1$ h. (b) $t = 4$ h. (c) $t = 11$ h. (d) $t = 12$ h.

area near offshore under the marine transportation accident of spent fuel on July 1 is greater than that on December 1. In addition, the vortex effect would cause the accumulation of radionuclides near the vortex besides limiting the dispersion range, which is not conducive to dilution of radionuclides by seawater and postaccident disposal.

3.3. Evolution of Maximum Radionuclide Concentration near Shore. Considering the effect of radioactive pollutant on the shore, evolution of maximum concentration of ^{137}Cs near shore in 12 hours is shown in Figure 9, and the red solid line and the blue solid line express the maximum concentration of ^{137}Cs near shore on July 1 and December 1, respectively. The red dashed line expresses the maximum permission value of ^{137}Cs in seawater. The maximum concentration of ^{137}Cs near shore arises at $t = 4$ h on July 1 (44532 Bq·m^{-3}), which is far more than the maximum permission value in seawater. However, compared with the maximum concentration of ^{137}Cs near shore on July 1, it is more approaching or exceeding the maximum permission value after $t = 8$ h on December 1. This means there is more and more radionuclide accumulation near shore on December 1 according to Figures 8(c) and 8(d).

In order to analyze detailed evolution of the maximum concentration near shore, Figures 8–10 illustrate the

maximum concentration of ^{137}Cs near shore in different time periods with 12 hours in 4 figures, from Figures 10(a)–10(d). Figure 10(a) shows the distribution of ^{137}Cs at $t = 1$ h; Figure 10(b) shows the distribution of ^{137}Cs at $t = 4$ h; Figure 10(c) shows the distribution of ^{137}Cs at $t = 11$ h; Figure 10(d) shows the distribution of ^{137}Cs at $t = 12$ h.

From Figure 10(a), there is almost no contaminant near shore for DBNPP in 1 hour on July 1 and December 1. Over time, the east shore of DBNPP would be contaminated gradually by radioactive pollutant, and the maximum concentration of ^{137}Cs near shore located opposite Xuzhou islands has exceeded the permission value in 4 hours on July 1 (as shown in Figure 10(b)) according to Figure 9. However, compared with the maximum concentration of ^{137}Cs near shore on July 1, it is greater at $t = 11$ h and $t = 12$ h after the accident condition on December 1 (as shown in Figures 10(c) and 10(d)).

The analysis of the Marine transportation scenario under accident condition, from the view of temporal and spatial variation, is fundamental to reduce the harmful radiation of the radionuclide leaked into the environment. Therefore, the prediction of the radionuclide dispersion in coastal water under accident condition is an effective solution for division of emergency response areas, so as to prevent the leaked radioactive pollutant from migrating to environment through water flow under nuclear accident.

4. Conclusions

Considering the continuous emission and dispersion for the radionuclide in coastal water flow, the distribution features with different time can be estimated in detail by the proposed model. There are different distributions of radionuclide under different hydrological conditions, with no effects of radiation hazard beyond maximum permission value on the west of the GBA within 12 hours under the boundary conditions in this work. One of the important factors in the distribution and migration of the radioactive pollutant in coastal water is that the effect of the vortex and wall leads to accumulation near the offshore, so as to contaminate areas for beaches, and vortex effect would cause the accumulation of radionuclides near the vortex besides limiting the dispersion range, which is not conducive to dilution of radionuclides by seawater and postaccident disposal. In addition, the distribution of radionuclide concentration is caused by different factors, such as the different transportation parameters, different water depth, different direction of water flow, and tidal conditions.

The scenario study of marine transportation for the radionuclide dispersion in coastal water under different hydrological conditions is the focus of this work. With consideration of the economy and timeliness, division of emergency response areas based on radionuclide dispersion simulation in coastal water under a marine transportation accident of spent fuel will be investigated in the next work. The decontamination area for beaches should be accurately differentiated in case of various hydrological conditions, which is able to help nuclear decision makers to evaluate the cost and effectiveness of the radiation decontamination, so as to provide more actual information regarding radioactive disposal after nuclear accident.

Data Availability

The data used to support the findings of the study can be obtained from the corresponding author upon request.

Conflicts of Interest

The authors declare no conflicts of interest.

Acknowledgments

This work was supported by the Open Project of Nuclear Power Safety Monitoring Technology and Equipment (Grant no. K-A2019.413), the Natural Science Foundation of the Anhui Higher Education Institutions of China (Grant no. KJ2020A0110), and the Outstanding Talent Support Program in University of Anhui Province. The authors are thankful for the V&V support by Institutional Center for Shared Technologies and Facilities of INEST, HFIPS, CAS.

References

[1] D. Barcelo, R. Periáñez, R. Bezhenar, I. Brovchenko, and G. D. With, "Modelling of marine radionuclide dispersion in IAEA MODARIA program: lessons learnt from the Baltic Sea and Fukushima scenarios," *The Science of the Total Environment*, vol. 569-570, pp. 594–602, 2016.

[2] K. Mori, K. Tada, Y. Tawara et al., "Integrated watershed modeling for simulation of spatiotemporal redistribution of post-fallout radionuclides: application in radiocesium fate and transport processes derived from the Fukushima accidents," *Environmental Modelling & Software*, vol. 72, pp. 126–146, 2015.

[3] L. Yue, X. Detao, L. Xinhua, Q. Shoukang, and H. Zhengzhong, "Discussion on the present situation of spent fuel transportation in China," *Radiation Protection*, vol. 36, pp. 31–46, 2016.

[4] M. Yun, R. Christian, G. K. Bo et al., "A software tool for integrated risk assessment of spent fuel transportation and storage," *Nuclear Engineering and Technology*, vol. 49, 2017.

[5] M. Simonsen, O. C. Lind, Ø. Saetra et al., "Coastal transport of river-discharged radionuclides: impact of speciation and transformation processes in numerical model simulations," *The Science of the Total Environment*, vol. 669, pp. 856–871, 2019.

[6] L. Chen, C. Chen, X. Zheng, H. Lin, Y. Yin, and P. Long, "Simulation of radionuclide diffusion in a dry storage of spent fuel under accident condition," *Progress in Nuclear Energy*, vol. 108, pp. 152–159, 2018.

[7] H. Kawamura, T. Kobayashi, A. Furuno, I. Teiji, and Y. Ishikawa, "Preliminary numerical experiments on oceanic dispersion of 131I and 137Cs discharged into the ocean because of the Fukushima Daiichi nuclear power plant disaster," *Journal of Nuclear Science and Technology*, vol. 48, 2011.

[8] D. Tsumune, T. Tsubono, M. Aoyama, and K. Hirose, "Distribution of oceanic 137Cs from the Fukushima Dai-Ichi nuclear power plant simulated numerically by a regional ocean model," *Journal of Environmental Radioactivity*, vol. 111, 2012.

[9] C. Dufresne, C. Duffa, V. Rey, and R. Verney, "Hydro-sedimentary model as a post-accidental management tool: application to radionuclide marine dispersion in the Bay of Toulon (France)," *Ocean & Coastal Management*, vol. 153, pp. 176–192, 2018.

[10] Z. Li, T. Zhou, B. Zhang, G. Si, and S. M. Ali, "Research on radionuclide migration in coastal waters under nuclear leakage accident," *Progress in Nuclear Energy*, vol. 118, 2020.

[11] P. Bailly du Bois, F. Dumas, L. Solier, and C. Voiseux, "In-situ database toolbox for short-term dispersion model validation in macro-tidal seas, application for 2D-model," *Continental Shelf Research*, vol. 36, pp. 63–82, 2012.

[12] S. Ben Hamza, S. Habli, N. Mahjoub Saïd, H. Bournot, and G. Le Palec, "Simulation of pollutant dispersion of a free surface flow in coastal water," *Ocean Engineering*, vol. 108, pp. 81–97, 2015.

[13] W. Wen, Y. Yuhan, and S. Dehai, "Study on the tidal dynamics in Daya Bay, China–Part I. Observation and numerical simulation of tidal dynamic system," *Journal of Tropical Oceanography*, vol. 36, pp. 34–45, 2017.

[14] P. Gallagher, R. Marcer, C. Berhault, C. D. Jouette, and F. Salvatore, *Best Practice Guidelines for the Application of Computational Fluid Dynamics in Marine Hydrodynamics*, WS Atkins Consultants and members of the NSC, 2009.

[15] K. Sorensen, *Safe and Secure Transport and Storage of Radioactive Materials*, Woodhead Publishing, Sawston, UK, 2015.

[16] Y.-H. Koo, Y.-S. Yang, and K.-W. Song, "Radioactivity release from the Fukushima accident and its consequences: a review," *Progress in Nuclear Energy*, vol. 74, pp. 61–70, 2014.

[17] K. Connolly and R. Pope, *A Historical Review of the Safe Transport of Spent Nuclear Fuel*, 2016.

[18] T. Xiang-Hai and X. Da-Yi, "2D numerical simulation of tidal current in the sea around Naozhou Island based on shallow water equation," *Marine Environmental Science*, vol. 39, pp. 867–873, 2020, in Chinese.

[19] Commission, "Hydro meteorological data in 2020," 2020, http://www--dayawan--gov--cn.proxy.huizhou.gov.cn/hzdywhyyyj/gkmlpt/index#4274.

[20] Z. Chunling, X. Zitu, and X. Zhang, "The research on the environmental impact on nearby waters range at low-level radioactive waste water drain from the dayawan nuclear power station," *Nuclear Power Engineering*, vol. 8, pp. 55–66, 1987.

[21] J. Cai, K. F. Ip, C. Eze, J. Zhao, J. Cai, and H. Zhang, "Dispersion of radionuclides released by nuclear accident and dose assessment in the Greater Bay Area of China," *Annals of Nuclear Energy*, vol. 132, pp. 593–602, 2019.